Journal of Advanced Research xxx (xxxx) xxx

Contents lists available at ScienceDirect

Journal of Advanced Research

journal homepage: www.elsevier.com/locate/jare

Original Article

Exopolysaccharide from the yeast *Papiliotrema terrestris* PT22AV for skin wound healing

Masoud Hamidi [a,b], Oseweuba Valentine Okoro [a], Giuseppe Ianiri [c], Hafez Jafari [a], Khodabakhsh Rashidi [d], Saeed Ghasemi [e], Raffaello Castoria [c], Davide Palmieri [c], Cédric Delattre [f,g], Guillaume Pierre [f], Mahta Mirzaei [a], Lei Nie [a,h,*], Hadi Samadian [i,*], Amin Shavandi [a,**]

[a] *Université libre de Bruxelles (ULB), École polytechnique de Bruxelles-3BIO-BioMatter unit, Avenue F.D. Roosevelt, 50 - CP 165/61, 1050 Brussels, Belgium*
[b] *Department of Medical Biotechnology, Faculty of Paramedicine, Guilan University of Medical Sciences, Rasht, Iran*
[c] *Dipartimento Agricoltura, Ambiente e Alimenti, Università degli Studi del Molise, Campobasso, Italy*
[d] *Research Center of Oils and Fats, Research Institute for Health Technology, Kermanshah University of Medical Sciences, Kermanshah, Iran*
[e] *Department of Medicinal Chemistry, School of Pharmacy, Guilan University of Medical Sciences, Rasht, Iran*
[f] *Université Clermont Auvergne, Clermont Auvergne INP, CNRS, Institut Pascal, F-63000 Clermont-Ferrand, France*
[g] *Institut Universitaire de France (IUF), 1 rue Descartes, 75005 Paris, France*
[h] *College of Life Sciences, Xinyang Normal University, Xinyang 464000, China*
[i] *Research Center for Molecular Medicine, Hamadan University of Medical Sciences, Hamadan, Iran*

HIGHLIGHTS

- P. terrestris PT22AV as a new yeast was identified.
- The extracted EPS has antioxidant and antibacterial activities and could be biocompatible and hemocompatible.
- The EPS showed a dose-dependent wound healing effect using an *in vivo* full-thickness wound model.
- The EPS can be a promising biopolymer for wound healing acceleration and designing 3-dimensional scaffolds for biomedical applications.

GRAPHICAL ABSTRACT

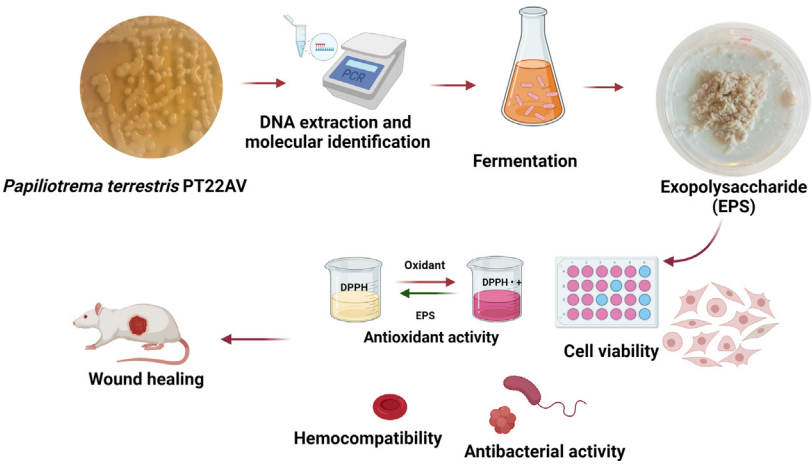

ARTICLE INFO

Article history:
Received 24 February 2022
Revised 9 June 2022
Accepted 21 June 2022
Available online xxxx

Keywords:
Exopolysaccharide (EPS)

ABSTRACT

Introduction: Exopolysaccharides (EPSs) are high-value functional biomaterials mainly produced by bacteria and fungi, with nutraceutical, therapeutic and industrial potentials.
Objectives: This study sought to characterize and assess the biological properties of the EPS produced by the yeast *Papiliotrema terrestris* PT22AV.
Methods: After extracting the yeast's DNA and its molecular identification, the EPS from *P. terrestris* PT22AV strain was extracted and its physicochemical properties (structural, morphological, monosaccharide composition and molecular weight) were characterized. The EPS's *in vitro* biological activities and

Peer review under responsibility of Cairo University.
* Corresponding authors.
** Corresponding authors.
E-mail addresses: nieleifu@yahoo.com (L. Nie), h30samadiyan@gmail.com (H. Samadian), Amin.Shavandi@ulb.be (A. Shavandi).

https://doi.org/10.1016/j.jare.2022.06.012
2090-1232/

Papiliotrema terrestris
Biological activity
Wound healing
Yeast

in vivo wound healing potential were also evaluated.
Results: The obtained EPS was water-soluble and revealed an average molecular weight (M_w) of 202 kDa. Mannose and glucose with 97% and 3% molar percentages, respectively, constituted the EPS. *In vitro* antibacterial activity analysis of the extracted EPS exhibited antibacterial activity (>80%) against *Escherichia coli*, *Staphylococcus aureus*, and *Staphylococcus epidermidis* at a concentration of 2 mg/mL. The EPS showed cytocompatibility against the human fibroblast and macrophage cell lines and the animal studies showed a dose-dependent wound healing capacity of the EPS with higher wound closure at 10 mg/mL compared to negative and positive control after 14 days.
Conclusion: The EPS from *P. terrestris* PT22AV could serve as a promising source of biocompatible macromolecules with potential for skin wound healing.

Introduction

Exopolysaccharides (EPSs) are natural extracellular metabolites secreted by microorganisms through their cellular membrane to the environment [1]. Although the mechanism of EPS production remains rudimentary, these metabolites are hypothesized to be generated from intracellular nucleotide sugars *via* chemical condensation reactions during microbial metabolic activity [2,3]. EPSs with inherent free radical scavenging, antimicrobial, and immunomodulatory activities have potential biomedical applications such as anticancer agents with bifidogenic characteristics, plasma expander, and pharmaceutical excipient [4–8]. For instance, EPSs could be used as immune modulators [9]. Mannose, glucose, galactose, and/or arabinose residues in polysaccharides have been shown to contribute to immunomodulatory action [10,11]. For example, β-glucans (βGs), containing only glucose residues, are one of the EPSs found in yeasts and filamentous fungi, and their immunostimulatory and immunomodulatory potential in the immune system has been intensively examined [8,10,12]. βGs, both branched and linear, are recognized as physiologically active chemicals known as biological response modifiers (BRMs). These glucans could be used to treat bacterial, viral, and protozoal diseases, and as anticancer medications [8,13,14]. Maity et al. extracted a water soluble βG from an edible mushroom *Entoloma lividoalbum* having molecular weight (M_W) ~2×10^5 Da. This βG activated macrophages in a dose-dependent manner, with maximum NO generation at 35 g/mL. Also, it was concluded that 12.5 μg/mL and 100 μg/mL are the optimum concentrations of this EPS for splenocytes and thymocytes proliferation, respectively [15].

βGs trigger signal transduction in polymorphonuclear phagocytes (e.g., macrophages, monocytes, dendritic cells, and natural killer cells) and neutrophils by interacting with pattern recognition receptors (PRRs) such as Dectin-1, complement receptor 3 (CR3), scavenger receptors, and lactosylceramide (LacCer) [8,16–18]. The PRRs' effectiveness is determined by the cell characteristics; for example, CR3 is mostly responsible for G-induced neutrophil regulation, whereas Dectin-1 is the most important G receptor on macrophages [8,19,20]. The activation of receptors by βG binding to the lectin site of the CR3 on phagocytes and NK cells enhances cytotoxicity against iC3b-opsonized target cells [8,21,22]. Dectin-1 recognizes βG on macrophages, which activates the downstream signaling pathway, which leads to phagocytosis, ROS production, microbial death, and cytokine secretion [8,20,23].

Moreover, different microbial EPSs have been shown to excite macrophages, which can kill pathogens directly through phagocytosis and indirectly protect the immune system by releasing cytotoxic chemicals [8,9]. It was previously shown that a α-glucan derived from *Hirsutella sinensis* may significantly improve macrophage phagocytosis and boost nitric oxide (NO), IL-1, IL-6, and tumor necrosis factor (TNF)-α production by activating the p38, JNK, and NF-B signaling pathways [24]. In another study, a water-soluble polysaccharide (MSP-3–1) from *Morchella sextelata* as α-glucan, which is primarily composed of mannose, glucose, and galactose was found to significantly boost macrophage RAW264.7 proliferation, phagocytosis, and NO generation [24]. In RAW 264.7 cells, Wang et al. discovered that EPS from *Trichoderma pseudokoningii* could dramatically increase NO, TNF-α, and IL-1 production as well as phagocytic activity. These findings imply that *T. pseudokoningii* EPS activates RAW 264.7 cells via NF-B and MAPK signaling pathways mediated by TLR4 and Dectin-1 [25].

EPSs have been shown to exhibit antibacterial properties against a wide range of pathogenic microorganisms in numerous studies [26], especially *Staphylococcus aureus*, *Enterococcus faecalis*, *Bacillus subtilis*, *Pseudomonas aeruginosa*, and *Escherichia coli* [27,28]. Many antibacterial mechanisms have been proposed in this regard, including preventing cell division and destroying DNA [29,30]. *Ganoderma applanatum* EPS, for example, was discovered to have antibacterial action against *S. aureus* [31]. Antimicrobial activity of EPSs from *Hirsutella* sp. against *B. subtilis* and *Micrococcus tetragenus* was also observed [32].

The application of EPSs depends mainly on their monomer composition and functional groups in their chemical structures [33,34]. For instance, the presence of α-(1 → 6) and α-(1 → 4) glycosidic linkages in pullulan enhances its adhesive characteristics and, thus, its capability to form fibers [35,36]. Similarly, the presence of β-glucan monomers in some EPSs enhances their antidiabetic effects due to the ability of β-glucans to transform to di- and trisaccharides, which have been reported to improve insulin sensitivity [37,38].

Our study sought to investigate EPS production by the yeast *Papiliotrema terrestris*, a basidiomycetous organism of the subphylum of *Agaricomycotina*, family *Tremellaceae* [39]. *P. terrestris* was selected due to its elevated anti-competitive behavior against a number of economically significant important fungal pathogens in post-harvest [40,41]. *P. terrestris* was also selected as a potential source of EPS due to its capability to resist factors that may inhibit EPS production (i.e. pathogens) through antagonistic effects against plant pathogens, a feature related to the high tolerance of *P. terrestris* to resist oxidative and other cellular (i.e. osmotic) stresses [39]. In the present study, a detailed taxonomic characterization of a new yeast strain of *P. terrestris*, PT22AV, was initially undertaken *via* rRNA gene sequencing. Subsequently, a fermentation operation for EPS production prior to its extraction, chemical characterization, and assessment of its biological activity via *in vitro* studies, was carried out. A full-thickness wound rat model was also used to evaluate the EPS's wound healing potential.

Materials and methods

Materials

Potato dextrose broth (PDB) was purchased from HiMedia, India. Agar was obtained from AppliChem, Germany. Sucrose was purchased from Fisher Chemical, Belgium. Ammonium sulfate ($(NH_4)_2SO_4$) was obtained from Acros Organics, USA. Potassium dihydrogen phosphate (KH_2PO_4) was purchased from Alfa Aesar, U.S.A. Methanol, magnesium sulfate heptahydrate ($MgSO_4{\cdot}7H_2O$), sodium chloride (NaCl), yeast extract, and Mueller Hinton Broth (MHB) were bought from Merck, Germany. Calcium chloride dehydrated ($CaCl_2{\cdot}2H_2O$) was purchased from Agro Organics, South Africa. Ethanol (96%) was purchased from Avantor®, Belgium. RealTime-Glo™ MT Cell Viability Assay kit was bought from Promega, USA. 1,1-diphenyl-2-picrylhydrazyl (DPPH) was obtained from Merck Sigma-Aldrich (St. Louis, MO, USA).

Ethics statement

All the *in vivo* studies are consistent with the National Institute of Health guidelines and the European Communities Council Directive (2010/63/EU) and are authorized by Kermanshah University of Medical Sciences (IR.KUMS.REC.1400.247).

Molecular identification of the microorganism

DNA extraction and polymerase chain reaction (PCR)

P. terrestris PT22AV, is a yeast isolated from olives in Molise (Italy) [42]. As yeast extract peptone dextrose (YPD) medium is recommended for routinely growing yeast cells [43], for DNA extraction, cellular pellet of *P. terrestris* PT22AV from a 2-day old YPD agar plate (Bacto-peptone 20 g/L, yeast extract 10 g/L, Dextrose 20 g/L) was inoculated in 20 mL of liquid YPD in a 50 mL flask and incubated or rotary shaking at 28 °C 160 rpm for 48 h. The culture was subsequently centrifuged using a 5810 Eppendorf (Hamburg, Germany) at 13000 rpm (5 min, 25 °C). The supernatant that resulted was disposed, and as reported in the literature, genomic DNA was isolated from the residual cells by a solvent mixture containing phenol/chloroform/isoamyl alcohol (50:48:2 v/v/v) [44]. For the amplification of the internal transcribed spacer (ITS) regions of *P. terrestris* PT22A, universal primers (ITS1 and ITS4) [45] were utilized. The PCR was carried out using a denaturation at 95 °C for 2 min, 33 cycles of denaturation at 95 °C for 30 s, annealing at 55 °C for 30 s, extension at 72 °C for 1 min, and a final extension at 72 °C for 5 min [46] using High Fidelity Phusion Taq. PCR reaction was mixed with DNA loading dye and run on a 1% agarose gel (v/w) at 70 V for 1 h, then visualized under UV light [47].

Phylogenetic study

For phylogenetic analysis, the ITS sequences of representative type strains of *Papiliotrema* species, namely *P. terrestris* CBS 10810, *P. laurentii* CBS 139, *P. aurea* CBS 318, *P. taeanensis* CBS 9742, *P. bandonii* CBS 9107, *P. rajasthanensis* CBS 10406, *P. pseudoalba* CBS 7227, and *P. flavescens*, were downloaded from GenBank. For other *P. terrestris* strains, the ITS region of strain LS28 was downloaded from GenBank (accession LR697098.1), while those of strains CBS 10811, CBS 10812, and CBS 10,813 were obtained from the Westerdijk Institute website. *Cryptococcus depauperatus* CBS 7841 was used as an outgroup. The sequences were aligned by the Muscle algorithm, and the MEGA 7 software program was employed to infer the evolutionary history through the Maximum Likelihood Phylogenetic Tree using the Tamura 3-parameter model (T92 + G) model [48].

Growth conditions for EPS production

According to the literature, a high C:N ratio and enough carbon and nitrogen supplies may enhance EPS formation by yeast cells and other microorganisms [49,50]. Then, for EPS extraction, cellular pellet of *P. terrestris* PT22AV from a 2-day old YPD agar plate was transferred with a loop on Potato Dextrose Agar (PDA) (as it has high C:N ratio (10:1)) [51] Petri dish and subsequently incubated at 28 °C for 24 h. The basal medium for getting more EPS yield comprised (g/L): sucrose, 30; yeast extract, 1; KH_2PO_4, 1; $(NH_4)_2SO_4$, 3; $MgSO_4{\cdot}7H_2O$, 0.5; NaCl, 0.1; and $CaCl_2{\cdot}2H_2O$, 0.01 [52]. The medium's pH was fixed to 5.3 at the beginning, and it was sterilized for 15 min at 121 °C. Batch culture containing 100 mL medium were used for microbial growth and EPS synthesis in a shaking incubator for 96 h (140 rpm, 28 °C) (New Brunswick Classic C24 Incubator Shaker, USA).

EPS extraction, purification, and characterization

EPS extraction and purification

A 10% (v/v) inoculum of *P. terrestris* PT22AV was made from a one-day culture in the basal culture medium (mentioned above) and incubated using the shaking incubator for 96 h (28 °C, 150 rpm). After incubation, the EPS-containing supernatant was collected by centrifugation at 8500 rpm for 30 min at 4 °C. From the supernatant, with adding dropwise cold ethanol with simultaneous stirring, the EPS was precipitated and then incubated overnight at 4 °C. Then, the precipitated EPS was 'twice washed' with ethanol to enhance EPS purity, followed by 20 min of 8500 rpm centrifugation at 4° [53,54]. To make dried EPS pellets, the EPS residue was dried at room temperature to a constant mass. After dissolving the EPS pellets in distilled water, the EPS solution was lyophilized (Christ freeze-dryer alpha I-5). The mass of the dried EPS was determined using a precision analytical balance (Sartorius, Germany), and the EPS yield was calculated (g/liter of culture medium). The phenol–sulphuric acid approach (using glucose as the standard) was applied to define the overall carbohydrate content of the EPS [55]. Additionally, protein content was concluded by the Bradford technique utilizing bovine serum albumin (BSA) as the reference [56]. Possible nucleic acid contaminations were assessed employing a spectrophotometer (Genesys™ 10S UV–Vis, USA) with the optical density (OD) of the EPS determined at the wavelengths of 260 nm and 280 nm.

Measurement of exopolysaccharide (EPS) solubility and intrinsic viscosity

The EPS solubility in distilled water, chloroform, and methanol was investigated according to the method previously described [57]. In brief, 1 mL of each solvent was blended with determined quantities (0.5, 1, 2, 3 and 4 mg) of the EPS in 2 mL microtubes and vortexed (1 min at room temperature).

A Lovis 2000 M/ME Rolling-ball viscometer (Anton Paar GmbH, Germany) was used to determine the intrinsic viscosity of the EPS. It was fitted with a glass capillary with a radius of 1.59 mm and a steel ball with a radius of 1.5 mm at a 30 angle. At 25 °C, viscosity was estimated for five concentrations of EPS in distilled water (0.5 to 4 mg/mL). Before the test, the solutions were filtered within a 0.45 mm Millipore filter.

The intrinsic viscosities, $[\eta]$ in mL/mg, of the EPS, were subsequently determined by calculating their reductions of viscosities

and extrapolating the associated concentrations to infinite dilution following the Huggins equation as follows;

$$[\eta] = \lim \eta_{red} \text{ as } C \to 0 \quad (1)$$

where η_{red} represents the reduced viscosity (mL/g), η_{sp} is the specific viscosity (dimensionless) and C is the EPS concentration (mg/mL).

Scanning electron microscopy

The surface morphology of the EPS was evaluated using a scanning electron microscope (SEM) (SU-70 Hitachi Ltd., Tokyo, Japan). In this work, 5 mg of the EPS was applied on SEM stubs using double-sided tape, followed by a layer of gold coating and observation at 10–20 kV accelerating voltage [58,59].

Physicochemical characterization

Fourier transform infrared (FTIR) spectrum of the EPS was acquired by means of PerkinElmer spectrophotometer system (PerkinElmer Inc., CA, USA) equipped with an attenuated total reflectance (ATR) for determination of its functional groups. 4 mg of the EPS was introduced to the cleaned ATR crystal surface and the generated spectral signals documented in the wavelength range of 400 to 4000 cm^{-1} [53,60].

The EPS sample was scanned with an X-Ray Diffractometer (XRD; Bruker ecoD8 advance Eco, Germany) in the range of 5°<2Θ < 60° with Cu Kα irradiation (k = 0.154060 nm) at 40 kV and 25 mhA to create XRD arrays at various ranges of two-theta angles (10–70). The diffractometer was run at a frequency of 1.2 per min, with a step size of 0.019 and a scan step time of 96.00 s [61,62].

Molecular weight determination

The chromatographic retention technique was used with a steric exclusion chromatography (SEC)-HPLC (Agilent 1100 Series, Agilent Technologies, Waldbronn, Germany) to estimate the M_w of the EPS. The SEC-HPLC was equipped by a TSKgel G3000PWXL (10 µm, 7.8 × 300 mm) and a TSKgel G5000PWXL (10 µm, 7.8 × 300 mm) connected with a differential refractometer (DRI) and preceded by a TSKgel PWXL pre-column (12 µm, 6.0 × 40 mm). Isocratic elution was carried out by means of 0.1 M $NaNO_3$ solution at a 1 mL/min flow rate at 30 °C. 20 µL Pullulan samples (M_w ranging from 1.3 kDa to 800 kDa) were injected as standard polysaccharides at 10 g/L. The EPS was injected at a concentration of 10 g/L and eluted as described above [53].

Monosaccharide composition determination

The monosaccharide composition of the EPS was determined using gas chromatography-mass spectrometry (GC–MS). Briefly, 1 mL of 2 M trifluoroacetic acid (TFA) was applied to 10 mg EPS to catalyze the preliminary hydrolysis of EPS to its monomers. The resulting mixture was then vortexed for 10 s and after that, a 90-min incubation period at 120 °C in a water bath was undertaken, followed by a solvent evaporation procedure in a nitrogen stream. The procedure of trimethylsilylation derivatization was carried out as described by Pierre et al. [63] and D-Glucose (D-Glc), D-Mannose (D-Man), D-Xylose, D-Galactosamine (D-GalN), (D-Xyl), D-Galactose (D-Gal), D-Glucuronic acid (D-GlcA), D-Glucosamine (D-GlcN), D-Galacturonic acid (D-GalA), L-Rhamnose (L-Rha), L-Arabinose (L-Ara), and L-Fucose (L-Fuc) were used as internal standards. Agilent 6890 Series GC System, connected with an Agilent 5973 Network Mass Selective Detector, were utilized for GC–MS analysis applying electron impact (EI) ionization as previously reported in the literature [64].

In vitro biological activities

Antibacterial activity

Based on the literature, the main bacterial agents responsible for nosocomial and skin infections belong to *Staphylococci*, a wide variety of Enterobacteriaceae, *Pseudomonas* species, *Acinetobacter* species [65–68]. So, Gram-positive (Staphylococcus aureus ATCC 25,923 and Staphylococcus epidermidis ATCC 14990) and Gram-negative (Escherichia coli ATCC 27195) bacteria were selected to examine the antibacterial activity of the EPS sample based on the protocol provided by clinical and laboratory standards institute (CLSI) [69]. Briefly, Muller–Hinton broth (MHB) medium was incubated at 37 °C until an absorbance value of 0.5 McFarland corresponds to a cellular concentration of 1.5 × 10^8 CFU/mL [69]. The inoculum was diluted in the MHB medium to reach a final concentration of approximately 1 × 10^6 CFU/mL [69]. The sterile lyophilized EPS was solubilized in MHB medium at a concentration of 2 mg/mL. Different concentrations of samples (2–2000 µg/mL) were analyzed via 2-fold serial dilution in 96 well plates. Bacterial growth was assessed by determining its absorbance at 600 nm following incubation at 37 °C (24 h). The antibacterial activity was estimated by the subsequent equation:

$$Antibacterial\ activity(\%) = \left(\frac{A_c - A_s}{A_c}\right) \times 100 \quad (2)$$

where the absorbance of the control (MHB medium) and sample at 600 nm, respectively, are Ac and As. [70]. All experiments were done in triplicates. To examine whether there was a significant differences between treatments and concentrations, the one-way ANOVA was performed.

Antioxidant activity

Natural antioxidants have recently received a lot of interest from scientists and the general public because of their potential to replace synthetic antioxidants in maintaining human health and preventing and treating diseases [4]. Polysaccharides, especially EPSs, have been identified as promising antioxidants that could be exploited to generate effective and non-toxic pharmaceuticals for a variety of uses, including wound healing [71,72]. One of the most extensively used methods for screening antioxidant chemicals is the 2,2-diphenyl-1-picryl-hydrazyl-hydrate (DPPH) test [73]. Thus, the EPS sample's antioxidant activity was quantified at various concentrations (0.1, 0.25, 0.5, 1, 2.5, and 5 mg/mL) by measuring its DPPH radical scavenging activity. L-ascorbic acid was used as the positive control. The DPPH activities of the different EPS concentrations were investigated using the method reported in the literature [74]. Briefly, 150 µL of the EPS solution (in water) was blended with 150 µL of methanol solution of DPPH (100 µM) and transferred into a 96-well plate which was held in the dark at room temperature (40 min). The absorbance of the mixture was subsequently documented at 517 nm employing a UV–Vis Spectrophotometer (Microplate spectrophotometer, Epoch-BioTek, Winooski, USA), and the DPPH inhibition activity percent of the EPS solutions was determined by the equation (3);

$$Inibition\% = 1 - \frac{Abs_s - Abs_{sb}}{Abs_c - Abs_b} \times 100 \quad (3)$$

where Abs_s implies the absorbance of the sample (EPS in water + DPPH solution), Abs_{sb} indicates the absorbance of the blank sample (EPS in water + methanol), Abs_c stand for the absorbance of the control (methanol + DPPH) and the Abs_b is the absorbance of the blank (methanol only).

Hemocompatibility test

2.5 mL PBS (stock solution) was used to dilute 2 mL of anticoagulated human red blood cells (RBCs) and 200 μL of this mixture was used in the preparation of EPS solutions at various concentrations (1, 5, and 10 mg/mL). The blend was then maintained at 37 °C (60 min). The incubated RBCs + EPS solution was then centrifuged (1500 rpm, 10 min) and the absorbance of the supernatant test was determined at the wavelength of 545 nm by the Microplate Reader. The hemolysis percentage was then determined as follows [75,76];

$$\text{Hemolysis}\% = \frac{D_t - D_{nc}}{D_{pc} - D_{nc}} \times 100 \quad (4)$$

where D_t represents the absorbance of the supernatant sample, D_{nc} represents the absorbance of the negative control (RBCs diluted in PBS), and D_{pc} represents the absorbance of the positive control (water lysed RBCs).

Effect of the EPS on the viability of human fibroblasts and macrophages cell lines

Macrophage (U937, a pro-monocytic human myeloid leukaemia cell line, ATCC:CRL-1593.2) and human fibroblast (ATCC:CCL-186) cell lines were treated by various concentrations of the EPS (250, 500, 750, 1000, and 2000 μg/mL), and their viabilities were assessed using a luminescence test based on adenosine triphosphate quantification (CellTiter-Glo, Promega, Wisconsin). Cell lines passage 19 were cultured, respectively in Roswell Park Memorial Institute Medium (RPMI-1640) and in Dulbecco's modified Eagle's medium (DMEM) (LONZA, Verviers, Belgium) complemented with Fetal Calf Serum (FCS) (10% v/v), 1% (w/v) Penicillin-streptomycin (Gibco, Rockville, MD, USA) and kept at 37 °C, in a 5% CO_2-humidified atmosphere. When the cells reached 80% confluency, they were plated in triplicate in a white 96-well plate with 10^4/well density [77]. The human fibroblast and macrophage cells were - treated with 50 μL of the EPS samples (dissolved in the cell culture media) and 50 μL of RealTime-Glo™ MT Cell Viability kit components. Control cells were cultured in a media not containing the EPS. The viability of cells was subsequently evaluated according to manufacturer instruction by monitoring Luminescence on a Microplate luminometer (Centro XS LB 960-Berthold) set at 0, 16, 24, 40 and 48 h.

Wound healing studies

The full-thickness wound healing effects of the EPS were assessed *in vivo* employing 30 adult male Wistar rats (2 months old, weighing 200–220 g). The rats were initially divided at random into five groups (six rats per group) as follows; Group1, without treatment (the negative control group), Group 2, treated with commercial phenytoin cream 1% (the positive control group), and Groups 3, 4 and 5, handled with EPS solutions at the concentrations of 1, 5, and 10 mg/mL (test groups), respectively. General anesthesia containing a mixture of Ketamine 5% (70 mg/kg) and Xylazine 2% (6 mg/kg) was administered using an intraperitoneal injection (IP). The rats' back hair was shaved, and the skin was sterilized using 70% (v/v) ethanol [78]. A circular full-thickness skin excision (diameter of 1 cm) was performed on the back of each rat. The created wounds were treated (immediately after the wound induction) every other day according to the above-mentioned grouping and evaluation was based on the wound closure percent and histopathological evaluations. The microscopic appearance of the wounds was monitored during the healing process and the wound closure percent (*WC%*) was calculated as follows;

$$WC\% = 1 - \frac{OP_w}{IP_w} \times 100 \quad (5)$$

where OP_w denotes the open wound area, in m^2 and IP_w denotes the initial wound area, in m^2.

The histopathological assessments were conducted using the H&E and MT staining at 14 d after treatment. Briefly, the rat models were euthanized using an IP injection of a mixture of Ketamine/Xylazine (150/20 mg per kg). The wound zone was harvested, prepared in buffered formalin (10%, pH: 7.4) for 48 h, blocked, sectioned, and stained by Hematoxylin and Eosin (H&E) and Masson's trichrome (MT) methods. The results were observed and interpreted by an independent pathologist by means of a light microscope (Olympus, Tokyo).

Statistical analysis

Statistical investigation regarding the relationship between *WC %* with different time intervals and different treatment groups were conducted using Minitab ®20.4 software. Data analysis and all graphs (*in vitro* and *in vivo*), were generated using GraphPad Prism 9.0.0 (GraphPad Software, LLC, USA). The two-way ANOVA test with Dunnett's multiple comparisons was used to check for the significance. When $p < 0.05$, a statistically significant difference was indicated between the groups.

Results and discussion

Morphological and genome characteristics

P. terrestris PT22AV grown in YPD rich media produce yellow/orange and smooth colonies (Fig. 1a), while in PDA medium *P. terrestris* PT22AV colonies appeared as white/yellow, bright, and highly mucoid (Fig. 1b) at temperatures ranging from 15 °C and 30 °C. The mucoid part in the PDA agar represents the EPS produced by *P. terrestris* PT22AV on a Petri dish (Fig. 1b). Because of the undefined composition of the nutrients present in this media, at the moment it is unclear how the EPS production is regulated at a physiological level.

The ITS region indicated that PT22AV strain shares 100% similarity with the type of strain of *P. terrestris* CBS 10,810 as displayed in the maximum-likelihood (ML) phylogenetic tree with log-likelihood tree of −2176.40 (Fig. 1c). PT22AV strain was also closely related to *P. flavescens* and *P. aurea*, and is distinct from the *P. laurentii* subclade, in accordance with previous results [79].

EPS production and characterization

EPS production, solubility, and intrinsic viscosity

The total yield of the EPS extracted from the *P. terrestris* PT22AV grown in the basal medium was 780 ± 1.8 mg/L and composed mainly of carbohydrates (93 %), proteins (0.3 %), and nucleic acids (0.1%), as validated by their OD at 260 and 280 nm. Thus the EPS is predominantly comprised of carbohydrates, proteins, nucleic acids (94.6 %), and a low portion (5.4 %) of ash and non-carbohydrate substituents, for instance sulfate, pyruvate, methyl, or acetyl groups [80–83].

This observation is in agreement with the other studies. For example, Seviri et al. reported that the EPS from *R. babjevae* that was estimated by phenol–sulphuric acid technique, was composed of carbohydrate (78%) and protein (1.1%) [52]. Furthermore, the EPS from *R. mucilaginosa* sp. GUMS16 was primarily constituted of carbohydrates (61.7%), with relatively minor amounts of nucleic acid (0.7%) and protein (0.8%) [53].

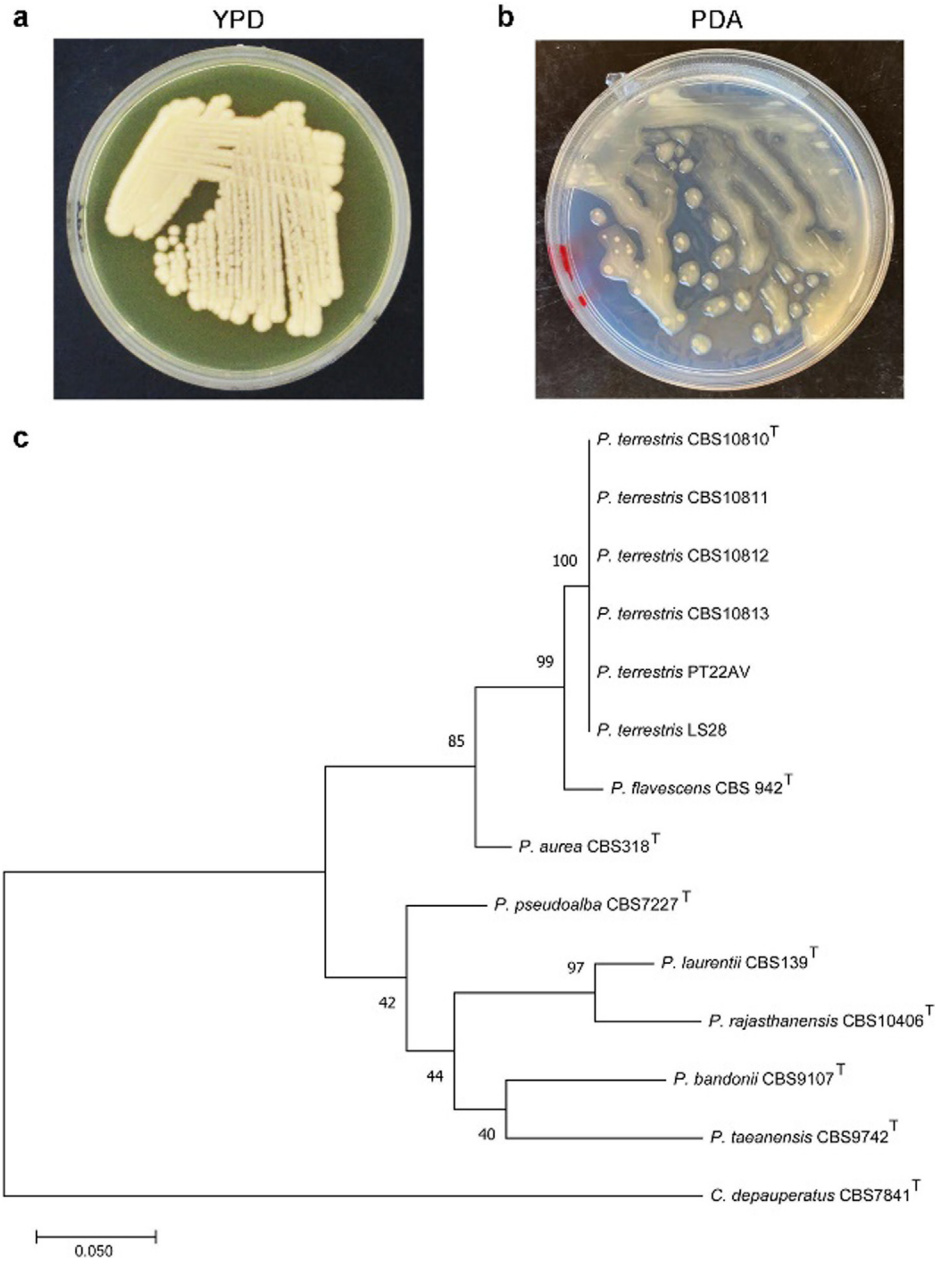

Fig. 1. *Papiliotrema terrestris* strain PT22AV streaked onto YPD (a) and PDA (b) plates and incubated at 28 °C for 10 days (c) Phylogenetic relation of representative *Papiliotrema* species based on ITS analysis. For the investigation of *P. terrestris,* numerous strains were included. By means of the Maximum Likelihood approach and the Tamura 3-parameter model, the evolutionary history was inferred. The highest log-likelihood tree (-2176.40) is presented. Next to the branches is the proportion of trees in which the related taxa clustered together. The initial tree(s) for the heuristic search were automatically created by employing the Neighbor-Join and BioNJ algorithms to a matrix of pairwise distances computed by the Tamura 3 parameter model, and then picking the topology with the maximum log-likelihood value. The evolutionary rate differences between sites were modeled using a discrete Gamma distribution [5 categories (+G, parameter = 0.2909)]. The branch lengths are calculated in the number of substitutions per site, and the tree is depicted to scale. There were 14 nucleotide sequences in this analysis. The total number of positions in the final dataset was 583.

Several yeast strains can produce EPSs. For example, *Candida boidinii* has been found to produce <1 g/L of EPS [84]. A *Rhodotorula glutinis* strain produced EPS at a yield of about 0.8 g/L [85]. Furthermore, after 14 days of fermentation, the maximum amount of EPS produced by *Antrodia cinnamomea* (an edible Basidiomycete) was 0.49 g/L [86]. Thus, it can be concluded that, in addition to the type of strain, factors such as culture conditions and the medium composition can affect the production of the EPSs and they need to be optimized. Therefore, in future studies, it is hoped that the production of the EPS by *P. terrestris* PT22AV be scaled up for industrial applications [52].

At 22 °C, the EPS was soluble in water but insoluble in the organic solvents (chloroform and methanol). Polysaccharides have a wide range of solubility: some are insoluble in water, such as cellulose; some are only soluble in hot water, such as starch; and some, like pullulan, gum Arabic and most of microbial EPSs, are easily dissolved in cold water [87,88]. Polysaccharides include many OH groups, with a significant attraction for water molecules. However, hydrogen bonding results in a strong contact between polysaccharide molecules. As a result, understanding polysaccharide solubility requires a balance of molecule–molecule and molecule-water interactions [87]. The interactions between

polysaccharide molecules and water molecules are energetically beneficial for soluble polysaccharides, and the solvent forms a solvating envelope around the polymer chain, keeping the polysaccharide molecules apart [87]. Thus the observed solubility of the EPS was consistent with previous reports [52,53]. For example, EPSs produced from Rhizobium tropici SEMIA 4077 and Rhodosporidium babjevae were soluble in water however insoluble in the organic solvents (methanol, chloroform, and toluene) [52,57]. Similarly, EPS extracted from *R. mucilaginosa* sp. GUMS16 was soluble in distilled water but not chloroform [53].

The intrinsic viscosity of the isolated EPS was 0.16 mL/mg. The intrinsic viscosity of the EPS was lower than commercial polysaccharides that range from 0.5 to 5 mL/mg [89]. The low intrinsic viscosity of the EPS from *P. terrestris* PT22AV implies that its solution in water will exhibit poorer thickening than commercial polysaccharides in that intrinsic viscosities will require higher concentrations (> 4 mg/mL) of the EPS solution.

Surface morphology, FTIR spectrum, and XRD pattern

As presented in Fig. 2a, the EPS has porous surface structure with grain-like elongated structural units. These grain-like elongated structural units, have been reported to be responsible for the compactness of polysaccharides [90]. Notably, these surface properties of the EPS are consistent with the previous reports. For example, EPSs from *R. mucilaginosa* sp. GUMS16 and *R. babjevae* exhibited similar porous surfaces with grain-like structural unit characteristics [52,53].

FTIR has proven to be an effective method for tracking structural changes in biopolymers [91,92]. Fig. 2b shows the FTIR spectrum of the EPS. The observed broad peak at 3252 cm^{-1} is related to the stretching vibrations of O–H [93–95] and the sharp peak noticed at the 2928 cm^{-1} is because of the stretching vibrations of C–H indicating the presence of the CH_3 functional group [94–96]. The peaks at 1638 cm^{-1} and 1406 cm^{-1} can be attributed to C = O stretching and C–H bending vibrations of carboxylic and CH_3 or/and CH_2 functional groups, respectively [93,94,97]. Sharp peaks at 1070 cm^{-1} and 599 cm^{-1} indicate the existence of C—O—C bonds and glycosidic linkages, respectively [96,97]. The FTIR spectroscopy showed that the EPS contains CH_3, CH_2, and carboxylic functional groups and glycosidic linkages [96,97] and it is in consistent with other microbial EPSs. For example, it was reprtred that EPSs such as xanthan molecules are identified by peaks at wave numbers of 3400 cm^{-1} (–OH stretch), 2940 cm^{-1} (C–H stretch) and 1040 cm^{-1} (C–O bond from the alcohol group) [98]. Moreover, it might be concluded that carboxyl groups in the EPS may act as binding sites for divalent cations [91,98].

In Fig. 2c, the XRD pattern of EPS depicts five intensive distinct sharp peaks between 10° – 40°. These sharp peaks were observed at

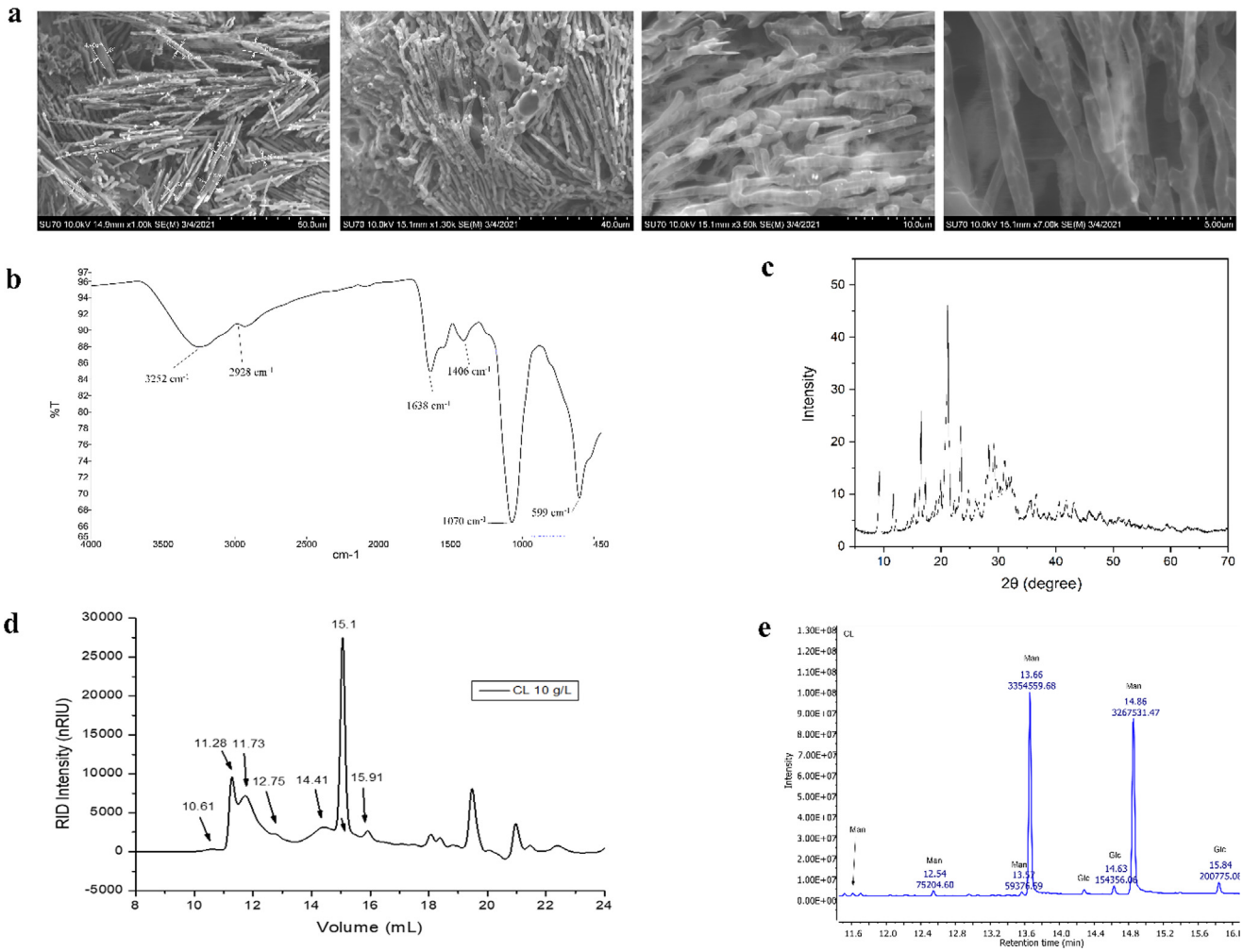

Fig. 2. **(a)** SEM images displaying the surface morphology of the EPS generated by *P. terrestris* PT22AV at × 1000 (A), ×1300 (B), ×3500 (C) and × 7000 (D) magnifications. (**b**) FTIR spectrum of the EPS produced by *P. terrestris* PT22AV. (**c**) XRD pattern of the EPS extracted from *P. terrestris* PT22AV. **(d)** Steric exclusion chromatography (SEC)-HPLC of the EPS from *P. terrestris* PT22AV for MW estimation. As it can be seen, it is a polydisperse fraction that is several families with several MW can be observed. As a result, we have a mixture of high and low molecular weight polymers. **(e)** GC–MS chromatogram of the EPS from *P. terrestris* PT22AV for analysis of monosaccharide composition.

16.52°, 21.18°, 23.45°, 28.36°, and 29.22° and are related to inter planar spacing (d-spacing) of 5.36 Å, 4.20 Å, 3.79 Å, 3.14 Å and 3.04 Å, respectively. The XRD investigation showed that the EPS holds an almost semi-crystalline nature with the crystallinity index (CI) of 0.442. This finding is in agreement with reports on EPSs isolated from *Leuconostoc lactis* KC117496 and *Weissella confusa* MD1 [99].

Molecular weight and monosaccharide composition analysis

As displayed in Fig. 2d, the average M_w of the EPS sample was 202 kDa. It was also determined via GC–MS (Fig. 2e) that mannose constitutes the main monosaccharide unit (97% on a molar basis) present in the EPS, with the residual component being glucose. The M_w evaluation revealed that the EPS contains a high content of mannose monosaccharide units since this M_w is comparable to the M_w of mannan I and mannan II (i.e. mannose sugars) from *Rhodotorula acheniorum* MC that were 310 kDa and 249 kDa, respectively [100]. Moreover, the CI value obtained from XRD analysis is matched with the value reported for the mannan EPSs (i.e. EPSs containing only monomeric mannose units) characterized by semi-crystalline structures (CI of 0.5) [99].

In vitro biological activity

Antibacterial activity

The antibacterial activity of the EPS was investigated against *E. coli, S. aureus and S. epidermidis* (Fig. 3a). EPS at the concentration of 2 mg/mL inhibited 89.46 ± 1.8 %, and 84.07 ± 0.5 % of bacterial growth against *E. coli* and *S. aureus,* respectively. Besides, the antibacterial activity of the EPS was more effective on *S. epidermidis* compared to *E. coli* and *S. aureus* with the antibacterial activity of 92.56 ± 3 % and 88.78 ± 2.5 % against *S. epidermidis* at the concentration of 2 and 1 mg/mL, respectively. According to the published literature, this is the first investigation on the antibacterial activity of the EPS produced in *Papiliotrema* genus.

Vazquez-Rodriguez et al. reported that when serial dilutions of the EPS from *R. mucilaginosa* UANL-001L were applied against *S. aureus* (ATCC 6538), a dose-dependent inhibitory action was detected. The EPS has the highest antibacterial action, inhibiting 60 % of bacterial growth at doses between 1000 and 2500 ppm. The EPS was also susceptible to *E.coli* (ATCC 11229) and *P. aeruginosa* (ATCC 27853) at 2000 and 2500 ppm, limiting bacterial growth by 27 % and 24 %, respectively [101]. In another study, the EPS from *Lacticaseibacillus rhamnosus* (isolated from human breast milk) was found to have significant antibacterial activity against *Salmonella enterica* serovar *Typhimurium* and *E. coli* [26]. When tested against *E. coli* and *S. aureus*, the EPS generated by *Lactiplantibacillus plantarum* C70 isolated from camel milk induced a 2–3 log reduction in viability [102]. The EPS from *Aspergillus* sp. DHE6 revealed excellent antibacterial efficacy against the tested dangerous human pathogens in an agar diffusion assay (*S. aureus*, *B. subtilis*, *Bordetella pertussis* and *P. aeruginosa*) [5].

It is worth mentioning that in our future studies, we will undertake an experimental trial to optimize the minimum inhibitory concentration capable of reducing microbial growth of the species tested (using C50 and C90) according to the CLSI protocol. Also, some appropriate experiments will be planned to do in the future to determine the bactericidal or bacteriostatic action of EPS against the pathogenic bacteria tested.

Antioxidant activity

The antioxidant activity of the EPS at different concentrations (0.1–5 mg/mL) was studied based on DPPH radical scavenging activity (Fig. 3b). The results showed a positive relationship concerning the EPS concentrations and the DPPH radical antioxidant activity. Increasing the EPS concentration from 0.1 mg/mL to 5 mg/mL, improved the scavenging activity from 20% to 37%. The *in vitro* evaluations revealed a DPPH antioxidant activity for the EPS that may be because of its ability to prevent the creation of hydroxyl radicals *via* the hydrogen or electron abstraction procedure [103]. Furthermore, the strong abstraction effects of the hydrogen from mannose monosaccharide units in the EPS may be responsible for the observed DPPH radical scavenging activity [104–107]. A few further studies on the antioxidant properties of EPSs generated from yeasts have been published. For instance, Wang et al. described that the maximum scavenging level of superoxide anion and hydroxyl radicals by the EPS from *Rhodotorula* sp. RY1801 is 29% and 84%, respectively [108]. Similarly, EPSs produced by *R. mucilaginosa* sp. GUMS16 (28.7 ± 2.62% at the concentration of 7.5 mg/mL), *R. babjevae* (25.2 ± 1% at the concentration of 10 mg/ml), and *Rhodotorula minuta* IBRC-M 30,135 (21.8 ± 0.7%, at the concentration of 10 mg/ml) exhibited concentration-dependent DPPH radical scavenging activities [52,53,109].

Hemocompatibility test

The hemocompatibility of the EPS was examined at 3 distinct concentrations (1, 5, and 10 mg/mL) using an anticoagulated human blood (Fig. 3c). The findings indicated that at all tested concentrations of the EPS, there was significantly ($p < 0.0001$) less hemolysis (5–6%) compared to the positive control (distilled water), demonstrating that the EPS did not induce significant hemolysis or damage to human red blood cells (RBCs). The hemocompatibility results showed that even at the high concentration of the EPS (10 mg/mL), hemolysis was low (5.33 ± 0.4%) which comparable to the value of 5% reported in the literature [110]. Our result showed that the EPS did not have any adverse effect on the rupturing of RBCs [110]. Similarly, MBF-15 EPS obtained from *Paenibacillus jamilae* was also hemocompatible [111].

Cell viability assay

Cell viability is defined as the amount of healthy cells in a sample, and cell proliferation is an important property that can clarify the mechanisms underlying the survival or death of cells after exposure to toxic chemicals [112]. Different cell viability assays have been developed; some of these monitor metabolic activity, ATP content, or cell growth to offer a readout of cell health. In this study, cell viabilities were assessed using adenosine triphosphate quantification by means of RealTime-Glo™ MT Cell Viability kit.

The outcomes of the treatment of human fibroblast (ATCC:CCL-186) [Fig. 3d] and macrophage (U937, a pro-monocytic human myeloid leukaemia cell line, ATCC: CRL-1593.2) [Fig. 3e] cell lines with the EPS at concentrations ranging from 250 to 2000 μg/mL up to 48 h, are shown in the Fig. 3d&e. Based on the results, the EPS was cytocompatible at concentrations < 1000 μg/mL. Moreover, using a concentration of 1000 and 2000 μg/mL of EPS on fibroblast cell line, a higher cell viability value was noted than that of the control.

The cell viability results of the EPS are consistent with EPS cell toxicity results reported in the literature. For example, the EPS (100 to 1000 μg/mL) from *R. mucilaginosa* sp. GUMS16 (a novel cold-adapted yeast), was biocompatible toward human dermal fibroblast (HDF) cell line during 48 h [53]. In addition, the EPS (10 to 1000 μg/mL) from *Weissella cibaria* EIR/P2 did not have a toxicity effect against human periodontal ligament fibroblast cells (hPDLFCs) during 24 h and also showed proliferative effect on hPDLFCs [113]. In addition, Liu et al. [114], Wang et al. [115], and

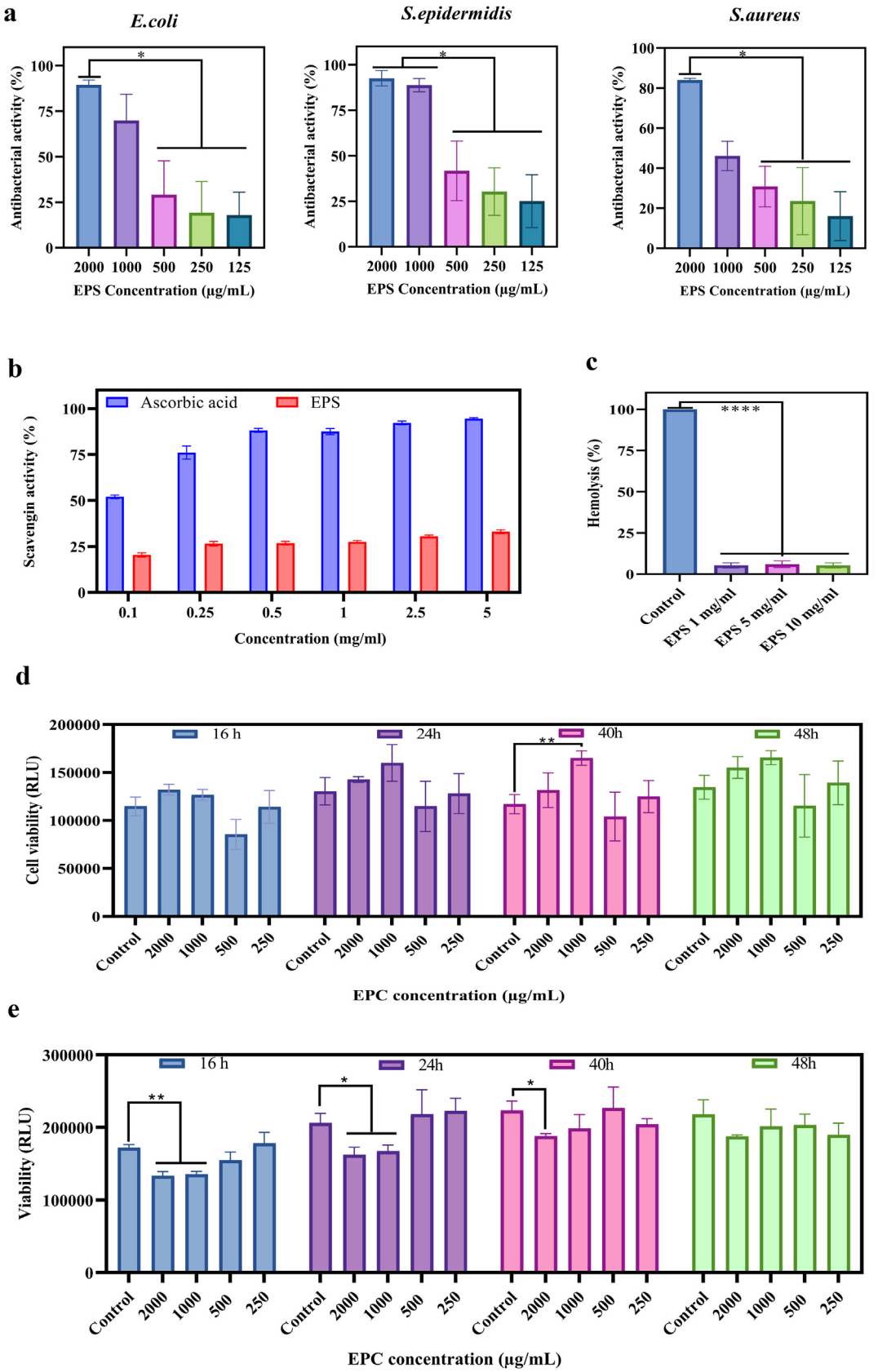

Fig. 3. **(a)** Antibacterial activity of EPS from *P. terrestris* PT22AV against *E. coli* ATCC 27195, *S. aureus* ATCC 25923, and *S. epidermidis* ATCC 14990. **(b)** The DPPH radical scavenging activity of the EPS from *P. terrestris* PT22AV with L-ascorbic acid as the positive control. (**c)** Hemocompatibility assay of the EPS from *P. terrestris* PT22AV on human red blood cells (RBCs). The results are stated as hemolysis percentage with respect to the positive control (distilled water). The values are the means of 3 independent tests performed in triplicate ± SD. (**d)** RLU-RealTime-Glo™ cell viability assay of the EPS from *P. terrestris* PT22AV on human fibroblast cell (ATCC: CCL-186) line after 16 h, 24 h, 40 h and 48 h of incubation. **(e)** RLU-RealTime-Glo™ cell viability assay of the EPS from *P. terrestris* PT22AV on human macrophage cell line (U937, a pro-monocytic human myeloid leukaemia cell line) after 16 h, 24 h, 40 h and 48 h of incubation. Each value is stated as mean ± SEM (n = 3) ($^{*}p < 0.05$, $^{**}p \leq 0.01$, $^{****}p \leq 0.0001$) vs. control group (without EPS). (For interpretation of the references to colour in this figure legend, the reader is referred to the web version of this article.)

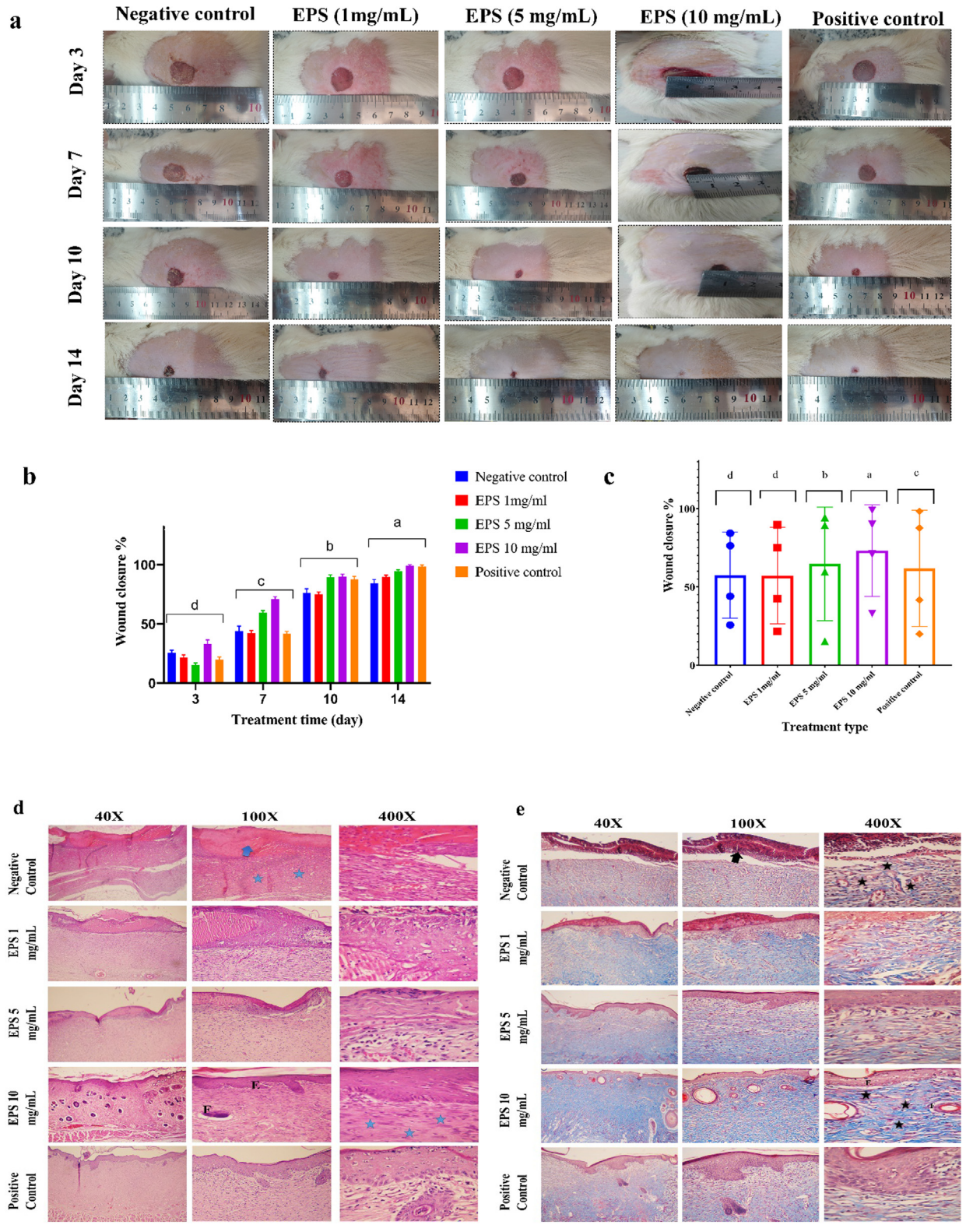

Fig. 4. **(a)** Contraction of excisional wounds in rats treated with three distinct concentrations of the EPS from *P. terrestris* PT22AV, sterile distilled water (as negative control group) and Phenytoin 1% cream (as positive control group). **(b)** Percentage wound closure (*WC%*) in controls and treated groups at different time intervals. Results are stated as *WC%* and are the mean ± SD of three individual tests. Data were investigated by means of a two-way ANOVA test, $^{a-d}$ bars that do not share a letter are significantly dissimilar at $p < 0.05$. **(c)** The relationship between *WC%* and different treatment groups. **(d)** Microscopic images of Hematoxylin and Eosin-stained tissues after 14-days post-surgery in three different magnifications. **(e)** Microscopic images of Trichrome Masson-stained tissues after 14-days post-surgery in three different magnifications. *Thick arrow*: Crusty scab, *E:* Epidermis layer, *F:* Hair follicle, *Stars in the negative control group:* Disordered connective tissue, *Stars in the tests group:* Ordered connective tissue.

Uhliariková et al. [116], found that the EPS from *Phomopsis liquidambari* NJUSTb1 (between 31.25 and 500 μg/mL), *Lactobacillus plantarum* JLK0142 (between 50 and 1000 μg/mL), and cyanobacterium *Nostoc* sp. (between 0 and 1000 μg/mL), respectively, had no toxicity effects on macrophage cell line (RAW 264.7). Moreover, Jiang et al. determined that the mannan EPS extracted from *P. pini*

displayed elevated macrophages-activating ability for enhanced phagocytosis *via* nitric oxide production, reactive oxygen species and tumor necrosis factor [117].

Wound healing

The wound healing effect of the EPS was assessed using a rat model for 14 d and macroscopic (percentage of wound closure (*WC%*)) and microscopic (histopathology) observations were recorded (Fig. 4a-e). Fig. 4b shows that the *WC%* for the negative and positive control groups were 85.3 ± 5.1% and 98.3 ± 4.2%, respectively. The results highlighted that the EPS facilitated a dose-dependent *WC%*, so that the highest *WC%* was 99.2 ± 4.0% when a treatment of EPS 10 mg/mL was administered. This highest *WC%* due to the EPS was comparable to the *WC%* due to the application of commercial phenytoin 1% cream. Fig. 4c represents the relationship between *WC%* and different treatment groups and indicates that the wound treated with EPS 10 mg/mL resulted in the best *WC%*.

The *WC* is a critical step in the wound healing process and can be used as a metric for the wound healing efficacy of a biomaterial. As shown in Fig. 4a-c, the treatment using the EPS accelerated the *WC%* and induced a dose-dependent *WC%*. The induced *WC%* upon the treatment using EPS 5 and 10 mg/mL at days 10 and 14, were statistically significant than the negative and EPS 1 mg/L ($p < 0.0001$). Similar to this study, *in vivo* wound healing ability of the EPS-Ca6 generated by *Lactobacillus sp.*Ca6 strain was tested by Trabelsi et al. On the 9th day, the WC% in rats treated with EPS-Ca6 was 89.4%, and on the 13th day, it was 97.91%. Also, they reported 77.16% and 80.62% of *WC%* in the physiological serum groups, respectively. There were no significant differences between the "Cytol Centella®" (positive control) and the EPS-Ca6 treated groups of rats [118]. Therefore, our finding is consistent with earlier research that the natural and complete *WC%* takes place by the 21st post-wounding day [118–120].

The histopathological evaluation using H&E and MT staining was performed to evaluate the wound healing progression under treatment with the EPS at the microscopic scale. Fig. 4 d&e show that in the negative control group (without treatment), the epidermal layer has not completely shaped after 14 d. Additionally, the infiltration of polymorphonuclear inflammatory cells (PMNs) was apparent in this group. Partial formation of the epidermal layer was observed under treatment with the EPS at concentrations of 1 mg/mL and 5 mg/mL. Although, in these groups (negative control, 1 mg/mL and 5 mg/mL treatment groups), the wound was covered by a crusty scab and the presence of PMNs was evident, indicating that the healing process has not been completed. In the group treated with EPS 10 mg/mL, the epidermal layer was formed, and sebaceous glands and hair follicles were observed (Fig. 4 d&e). MT staining was utilized to stain collagen fibers creation and distribution under treatments during the healing process. As shown in Fig. 4e, the highest collagen fibers synthesis and maturation were observed in EPS 10 mg/mL group.

To maximize regeneration and repair, skin wound healing is a multistage process involving various cellular and molecular interactions that affect cell behaviors and dynamic remodeling of extracellular matrix [121]. Inflammation, proliferation, and remodeling are the three steps that make up the wound healing process [122]. The proliferative and remodeling stages are less common in chronic wounds. The wound is still in the inflammatory phase, which inhibits tissue regeneration and prevents it from healing. Thus, targeting and treating the cellular and molecular causes of persistent wound inflammation may be an effective way to heal the wound [122]. Furthermore, the wound-healing process' efficacy is dependent on the balance of proinflammatory and pro-regenerative signals mediated by cytokines [123].

Platelets are triggered at the site of blood vessel rupture after skin damage and stimulate clot formation to limit blood loss. Platelets also release substances that attract immune cells from the surrounding bloodstream into the wound. The inflammatory phase begins at this point. The first to arrive are polymorphonuclear neutrophils, followed by monocytes that quickly develop into macrophages [122]. To clean the wound, neutrophils produce reactive oxygen species (ROS), proteases, and pro-inflammatory cytokines.

To clear the wound, macrophages will phagocytose bacteria and debris. The wound is disinfected and ready for tissue regrowth in the proliferative phase. Wound cells proliferate and move to rebuild the destroyed tissue. Endothelial cells, fibroblasts, and keratinocytes are examples of these cells [122].

Natural polysaccharides including microbial EPSs have received a lot of interest in recent years for their ability to modulate the inflammatory response during wound healing [124]. For example, Glucan wound treatment has been demonstrated to boost macrophage numbers, and promote fibroplasia, re-epithelialization, and wound strength [125,126]. Also, Xin et al. showed that in macrophages, treatment with water-soluble yeast (WSY) glucan increased the production of inflammatory mediators (prostaglandin E2 (PGE2) and nitric oxide (NO)) as well as pro-inflammatory cytokines (tumor necrosis factor (TNF)- and interleukin (IL)-6) significantly and dose-dependently. Furthermore, WSY glucan administration caused alterations in macrophage morphology and increased macrophage phagocytic activity as well as wound healing in keratinocytes [127]. It is critical to make sure that the material used to treat chronic wounds doesnot exacerbate the inflammatory response [122,128].

In the present study, the animal experiments showed dose-dependent wound healing effects under treatment with the EPS from *P. terrestris* PT22AV. The favorable wound healing effects of the EPS may be due to mannose facilitated recruitment of fibroblasts, keratinocytes, and macrophages under treatment *via* the mannose receptor-mediated migration [129]. Mannose may reduce the wound inflammation and the quantity of neutrophils due to its ability to inhibit hyaluronic acid (HA) by depleting uridine diphosphate N-acetylglucosamine as a raw component of HA bound to the CD44 receptor on neutrophils [130,131]. Mannose may also attach to the mannose receptor on macrophages inducing the transformation of M1 into phenotype M2 macrophages by stimulating the extracellular signal-regulated kinase (ERK) signaling route [132]. The phenotype M2 macrophages may accelerate the release of Interleukin 10, and transforming growth factor-beta (TGF-β), which reduces the inflammation phase of wound healing [133].

Conclusions

The present study investigated the yeast of *P. terrestris* PT22AV and its EPS product via an exploration of its structural, morphological, compositional, and biological properties as a precursory step to assessing the wound healing potential of the EPS. The PT22AV strain was completely similar to the more common strain of *P. terrestris* CBS 10,810 with the EPS product had antibacterial and antioxidant properties. The EPS from the PT22AV strain had the potential to enhance wound healing, thus constituting a promising biopolymer for the fabrication of wound dressings.

In the future, the authors anticipate more enthusiasm toward research into the development of PT22AV strain-EPS based wound dressings, with specific research activities focusing on the tuning of EPS to enhance its mechanical properties. It is the authors' opinion that future studies will also seek to explore the fundamental

molecular mechanisms of EPS-induced wound healing. This knowledge will enhance EPS transistion to clinical trials. Finally, we predict that the PT22AV strain will potentially serve as an economically competitive source of the EPS biopolymer due to its ease of culturing and EPS recovery.

CRediT authorship contribution statement

Masoud Hamidi: Conceptualization, Methodology, Formal analysis, Investigation, Validation, Funding acquisition, Writing – original draft, Writing – review & editing. **Oseweuba Valentine Okoro:** Investigation, Validation, Writing – review & editing. **Giuseppe Ianiri:** Investigation, Validation, Writing – review & editing. **Hafez Jafari:** Investigation, Validation, Writing – review & editing. **Khodabakhsh Rashidi:** Investigation, Writing – review & editing. **Saeed Ghasemi:** Investigation, Writing – review & editing. **Raffaello Castoria:** Investigation, Writing – review & editing. **Davide Palmieri:** Investigation, Writing – review & editing. **Cédric Delattre:** Investigation, Writing – review & editing. **Guillaume Pierre:** Investigation, Writing – review & editing. **Mahta Mirzaei:** Investigation, Writing – review & editing. **Lei Nie:** Investigation, Writing – review & editing. **Hadi Samadian:** Investigation, Supervision, Validation, Writing – review & editing. **Amin Shavandi:** Conceptualization, Validation, Resources, Supervision, Writing – review & editing, Visualization, Project administration.

Declaration of Competing Interest

The authors declare that they have no known competing financial interests or personal relationships that could have appeared to influence the work reported in this paper.

Acknowledgements

M.H would like to acknowledge the postdoctoral fellowship provided by the European Program IF@ULB. This project has received funding from the European Union's Horizon 2020 research and innovation programme under the Marie Skłodowska-Curie grant agreement No 801505. Also, *Giuseppe Ianiri* and *Raffaello Castoria* are supported by the PON AIM program Azione I.2 ''Attrazione e Mobilità dei Ricercatori''. The graphical abstract and Fig. 5 were created by BIORENDER (biorender.com). The auhtors also acknowledge the CARAMAT platform at the ULB for their assistance with SEM and XRD analyses.

References

[1] Wu Z, Yang Z, Gan D, Fan J, Dai Z, Wang X, et al. Influences of carbon sources on the biomass, production and compositions of exopolysaccharides from *Paecilomyces hepiali* HN1. Biomass Bioenergy 2014;67:260–9.
[2] Schmid J, Sieber V, Rehm B. Bacterial exopolysaccharides: biosynthesis pathways and engineering strategies. Front Microbiol 2015;6:496-.
[3] Osemwegie OO, Adetunji CO, Ayeni EA, Adejobi OI, Arise RO, Nwonuma CO, et al. Exopolysaccharides from bacteria and fungi: current status and perspectives in Africa. Heliyon 2020;6(6):e04205-e.
[4] Ragavan ML, Das N. Optimization of exopolysaccharide production by probiotic yeast *Lipomyces starkeyi* VIT-MN03 using response surface methodology and its applications. Ann Microbiol 2019;69(5):515–30.
[5] El-Ghonemy DH. Antioxidant and antimicrobial activities of exopolysaccharides produced by a novel *Aspergillus* sp. DHE6 under optimized submerged fermentation conditions. Biocatal Agric Biotechnol 2021;36:102150.
[6] Diao Y, Xin Y, Zhou Y, Li N, Pan X, Qi S, et al. Extracellular polysaccharide from *Bacillus* sp. strain LBP32 prevents LPS-induced inflammation in RAW 264.7 macrophages by inhibiting NF-κB and MAPKs activation and ROS production. Int Immunopharmacol 2014;18(1):12–9.
[7] Shyam KP, Rajkumar P, Ramya V, Sivabalan S, Kings AJ, Miriam LM. Exopolysaccharide production by optimized medium using novel marine *Enterobacter cloacae* MBB8 isolate and its antioxidant potential. Carbohyd Polym Technologies Applications 2021;2:100070.
[8] Hamidi, Okoro OV, Milan PB, Khalili MR, Samadian H, Nie L, et al. Fungal exopolysaccharides: Properties, sources, modifications, and biomedical applications. Carbohydr Polym 2022:119152.
[9] He C, Lin HY, Wang CC, Zhang M, Lin YY, Huang FY, et al. Exopolysaccharide from *Paecilomyces lilacinus* modulates macrophage activities through the TLR4/NF-κB/MAPK pathway. Mol Med Rep 2019;20(6):4943–52.
[10] Tian J, Zhang C, Wang X, Rui X, Zhang Q, Chen X, et al. Structural characterization and immunomodulatory activity of intracellular polysaccharide from the mycelium of *Paecilomyces cicadae* TJJ1213. Food Res Int 2021;147:110515.
[11] Figueiredo RT, Bittencourt VCB, Lopes LCL, Sassaki G, Barreto-Bergter E. Toll-like receptors (TLR2 and TLR4) recognize polysaccharides of *Pseudallescheria boydii* cell wall. Carbohydr Res 2012;356:260–4.
[12] Murphy EJ, Rezoagli E, Pogue R, Simonassi-Paiva B, Abidin IIZ, Fehrenbach GW, et al. Immunomodulatory activity of β-glucan polysaccharides isolated from different species of mushroom–A potential treatment for inflammatory lung conditions. Sci Total Environ 2022;809:152177.
[13] Geller A, Yan J. Could the induction of trained immunity by β-glucan serve as a defense against COVID-19? Front Immunol 2020;11:1782.
[14] Steimbach L, Borgmann AV, Gomar GG, Hoffmann LV, Rutckeviski R, de Andrade DP, et al. Fungal beta-glucans as adjuvants for treating cancer patients-A Systematic Review of Clinical Trials. Clin Nutr 2021;40:3104–13.
[15] Maity P, Sen IK, Maji PK, Paloi S, Devi KSP, Acharya K, et al. Structural, immunological, and antioxidant studies of β-glucan from edible mushroom *Entoloma lividoalbum*. Carbohydr Polym 2015;123:350–8.
[16] Brown GD, Gordon S. A new receptor for β-glucans. Nature 2001;413 (6851):36–7.
[17] Taylor PR, Tsoni SV, Willment JA, Dennehy KM, Rosas M, Findon H, et al. Dectin-1 is required for β-glucan recognition and control of fungal infection. Nat Immunol 2007;8(1):31–8.
[18] Chan G-C-F, Chan WK, Sze D-M-Y. The effects of β-glucan on human immune and cancer cells. J Hematol Oncol 2009;2(1):1–11.
[19] Baert K, Sonck E, Goddeeris BM, Devriendt B, Cox E. Cell type-specific differences in β-glucan recognition and signalling in porcine innate immune cells. Dev Comp Immunol 2015;48(1):192–203.
[20] Han B, Baruah K, Cox E, Vanrompay D, Bossier P. Structure-functional activity relationship of β-glucans from the perspective of immunomodulation: a mini-review. Front Immunol 2020;11:658.
[21] Ross GD, Větvička V, Yan J, Xia Y, Větvičková J. Therapeutic intervention with complement and β-glucan in cancer. Immunopharmacology 1999;42(1–3):61–74.
[22] Vetvicka V, Thornton BP, Ross GD. Soluble beta-glucan polysaccharide binding to the lectin site of neutrophil or natural killer cell complement receptor type 3 (CD11b/CD18) generates a primed state of the receptor capable of mediating cytotoxicity of iC3b-opsonized target cells. J Clin Invest 1996;98(1):50–61.
[23] Sato T, Iwabuchi K, Nagaoka I, Adachi Y, Ohno N, Tamura H, et al. Induction of human neutrophil chemotaxis by *Candida albicans*-derived β-1, 6-long glycoside side-chain-branched β-glucan. J Leukoc Biol 2006;80(1):204–11.
[24] Zhang Z, Shi M, Zheng H, Ren R, Zhang S, Ma X. Structural characterization and biological activities of a new polysaccharide isolated from *Morchella Sextelata*. Glycoconj J 2022:1–12.
[25] Wang G, Zhu L, Yu B, Chen K, Liu B, Liu J, et al. Exopolysaccharide from *Trichoderma pseudokoningii* induces macrophage activation. Carbohydr Polym 2016;149:112–20.
[26] Rajoka MSR, Jin M, Haobin Z, Li Q, Shao D, Jiang C, et al. Functional characterization and biotechnological potential of exopolysaccharide produced by *Lactobacillus rhamnosus* strains isolated from human breast milk. LWT 2018;89:638–47.
[27] Balouiri M, Sadiki M, Ibnsouda SK. Methods for in vitro evaluating antimicrobial activity: A review. J Pharm Anal 2016;6(2):71–9.
[28] Hamidi M, Ghasemi S, Bavafa Bighdilou B, Eghbali KD. Evaluation of antioxidant, antibacterial and cytotoxic activity of methanol extract from leaves and fruits of Iranian squirting cucumber (*Ecballium elaterium* (L.) A. Rich) Res J Pharmacogn 2020;7(1):23–9.
[29] DEMİR MS, YAMAÇ M. Antimicrobial activities of basidiocarp, submerged mycelium and exopolysaccharide of some native basidiomycetes strains. J Appl Biol Sci 2008;2(3):89-93.
[30] Wu MH, Pan TM, Wu YJ, Chang SJ, Chang MS, Hu CY. Exopolysaccharide activities from probiotic bifidobacterium: Immunomodulatory effects (on J774A. 1 macrophages) and antimicrobial properties. Int J Food Microbiol 2010;144(1):104–10.
[31] Osińska-Jaroszuk M, Jaszek M, Mizerska-Dudka M, Błachowicz A, Rejczak TP, Janusz G, et al. Exopolysaccharide from *Ganoderma applanatum* as a promising bioactive compound with cytostatic and antibacterial properties. Biomed Res Int 2014;2014.
[32] Li R, Jiang X-l, Guan H-s. Optimization of mycelium biomass and exopolysaccharides production by *Hirsutella* sp. in submerged fermentation and evaluation of exopolysaccharides antibacterial activity. Afr J Biotechnol 2010;9(2).
[33] Mahapatra S, Banerjee D. Fungal exopolysaccharide: production, composition and applications. Microbiol insights 2013;6:S10957.
[34] Gientka I, Błażejak S, Stasiak-Różańska L, Chlebowska-Śmigiel A. Exopolysaccharides from yeast: insight into optimal conditions for biosynthesis, chemical composition and functional properties? review. Acta Sci Pol Technol Aliment 2015;14(4):283–92.

[35] Prajapati VD, Jani GK, Khanda SM. Pullulan: An exopolysaccharide and its various applications. Carbohydr Polym 2013;95(1):540–9.
[36] Singh RS, Kaur N, Hassan M, Kennedy JF. Pullulan in biomedical research and development - A review. Int J Biol Macromol 2021;166:694–706.
[37] Cutting K. The cost-effectiveness of a novel soluble beta-glucan gel. J Wound Care 2017;26(5):228–34.
[38] Chen J, Raymond K. Beta-glucans in the treatment of diabetes and associated cardiovascular risks. Vasc Health Risk Manag 2008;4(6):1265.
[39] Castoria R, Miccoli C, Barone G, Palmieri D, De Curtis F, Lima G, et al. Molecular Tools for the Yeast *Papiliotrema terrestris* LS28 and Identification of Yap1 as a Transcription Factor Involved in Biocontrol Activity. Appl Environ Microbiol 2021;87(7):e02910–20.
[40] Lima G, De Curtis F, Castoria R, De cicco v.. Activity of the yeasts *Cryptococcus laurentii* and *Rhodotorula glutinis* against post-harvest rots on different fruits. Biocontrol. Sci Technol 1998;8(2):257–67.
[41] Castoria R, De Curtis F, Lima G, De Cicco V. β-1, 3-glucanase activity of two saprophytic yeasts and possible mode of action as biocontrol agents against postharvest diseases. Postharvest Biol Technol 1997;12(3):293–300.
[42] Curtis FD. Yeasts in the biological control against post- harvest fungal pathogens of fruit and vegetables: activities and mechanisms of action involved. National Libraries of Rome and Florence 1998.
[43] Ansbel F. Current Protocols in Molecular Biology (Current Protocols). NY and Wiley and Sons-Interscience, New York, NY: Brooklyn; 1987.
[44] Hoffman CS. Preparation of Yeast DNA. Curr Protoc Mol Biol: John Wiley & Sons, Inc.; 2001.
[45] White TJ, Bruns T, Lee S, Taylor J, Innis M, Gelfand D, et al. PCR protocols: a guide to methods and applications. 1990.
[46] Ros-Chumillas M, Egea-Cortines M, Lopez-Gomez A, Weiss J. Evaluation of a rapid DNA extraction method to detect yeast cells by PCR in orange juice. Food Control 2007;18(1):33–9.
[47] Green MR, Sambrook J. Analysis of DNA by agarose gel electrophoresis. Cold Spring Harbor Protocols 2019;2019(1):pdb.:top100388.
[48] Kumar S, Stecher G, Tamura K. MEGA7: Molecular Evolutionary Genetics Analysis Version 7.0 for Bigger Datasets. Mol Biol Evol 2016;33(7):1870–4.
[49] Díaz Bayona KC, Garcés LA. Effect of different media on exopolysaccharide and biomass production by the green microalga *Botryococcus braunii*. J Appl Phycol 2014;26(5):2087–95.
[50] Rahbar Saadat Y, Yari Khosroushahi A, Pourghassem GB. Yeast exopolysaccharides and their physiological functions. Folia Microbiol 2021;66(2):171–82.
[51] Mustafa U, Kaur G. Effects of carbon and nitrogen sources and ratio on the germination, growth and sporulation characteristics of Metarhizium anisopliae and Beauveria bassiana isolates. J Agric Res 2009;4(10):922–30.
[52] Mirzaei Seveiri R, Hamidi M, Delattre C, Sedighian H, Pierre G, Rahmani B, et al. Characterization and Prospective Applications of the Exopolysaccharides Produced by *Rhodosporidium babjevae*. Adv Pharm Bull 2020;10(2):254–63.
[53] Hamidi M, Gholipour AR, Delattre C, Sesdighi F, Mirzaei Seveiri R, Pasdaran A, et al. Production, characterization and biological activities of exopolysaccharides from a new cold-adapted yeast: *Rhodotorula mucilaginosa* sp. GUMS16. Int J Biol Macromol 2020;151:268–77.
[54] Choi IS, Ko SH, Lee ME, Kim HM, Yang JE, Jeong S-G, et al. Production, Characterization, and Antioxidant Activities of an Exopolysaccharide Extracted from Spent Media Wastewater after *Leuconostoc mesenteroides* WiKim32 Fermentation. ACS Omega 2021;6(12):8171–8.
[55] Dubois M, Gilles KA, Hamilton JK, Pt R, Smith F. Colorimetric method for determination of sugars and related substances. Anal Chem 1956;28 (3):350–6.
[56] Bradford MM. A rapid and sensitive method for the quantitation of microgram quantities of protein utilizing the principle of protein-dye binding. Analy Biochem 1976;72(1–2):248–54.
[57] Castellane TCL, Persona MR, Campanharo JC, de Macedo Lemos EG. Production of exopolysaccharide from rhizobia with potential biotechnological and bioremediation applications. Int J Biol Macromol 2015;74:515–22.
[58] Liu T, Zhou K, Yin S, Liu S, Zhu Y, Yang Y, et al. Purification and characterization of an exopolysaccharide produced by *Lactobacillus plantarum* HY isolated from home-made Sichuan Pickle. Int J Biol Macromol 2019;134:516–26.
[59] Gauri SS, Mandal SM, Mondal KC, Dey S, Pati BR. Enhanced production and partial characterization of an extracellular polysaccharide from newly isolated *Azotobacter* sp. SSB81. Bioresour Technol 2009;100(18):4240–3.
[60] Liao Y, Gao M, Wang Y, Liu X, Zhong C, Jia S. Structural characterization and immunomodulatory activity of exopolysaccharide from *Aureobasidium pullulans* CGMCC 23063. Carbohydr Polym 2022;119366.
[61] Rani RP, Anandharaj M, Sabhapathy P, Ravindran AD. Physiochemical and biological characterization of novel exopolysaccharide produced by *Bacillus tequilensis* FR9 isolated from chicken. Int J Biol Macromol 2017;96:1–10.
[62] Saravanan C, Shetty PKH. Isolation and characterization of exopolysaccharide from *Leuconostoc lactis* KC117496 isolated from idli batter. Int J Biol Macromol 2016;90:100–6.
[63] Pierre G, Zhao J-M, Orvain F, Dupuy C, Klein GL, Graber M, et al. Seasonal dynamics of extracellular polymeric substances (EPS) in surface sediments of a diatom-dominated intertidal mudflat (Marennes–Oléron, France). J Sea Res 2014;92:26–35.
[64] Benaoun F, Delattre C, Boual Z, Ursu AV, Vial C, Gardarin C, et al. Structural characterization and rheological behavior of a heteroxylan extracted from *Plantago notata Lagasca* (Plantaginaceae) seeds. Carbohydr Polym 2017;175:96–104.
[65] Agaba P, Tumukunde J, Tindimwebwa J, Kwizera A. Nosocomial bacterial infections and their antimicrobial susceptibility patterns among patients in Ugandan intensive care units: a cross sectional study. BMC Res Notes 2017;10 (1):1–12.
[66] Tolera M, Abate D, Dheresa M, Marami D. Bacterial nosocomial infections and antimicrobial susceptibility pattern among patients admitted at Hiwot Fana Specialized University Hospital. Eastern Ethiopia Adv Med 2018;2018:2127814.
[67] Halstead FD, Thwaite JE, Burt R, Laws TR, Raguse M, Moeller R, et al. Antibacterial activity of blue light against nosocomial wound pathogens growing planktonically and as mature biofilms. Appl Environ Microbiol 2016;82(13):4006–16.
[68] Tian L, Sun Z, Zhang Z. Antimicrobial resistance of pathogens causing nosocomial bloodstream infection in Hubei Province, China, from 2014 to 2016: a multicenter retrospective study. BMC public health 2018;18(1):1–8.
[69] Wikler MA. Methods for dilution antimicrobial susceptibility tests for bacteria that grow aerobically : approved standard. CLSI (NCCLS) 2006;26: M7-A.
[70] de Nova PJ, Carvajal A, Prieto M, Rubio P. In vitro susceptibility and evaluation of techniques for understanding the mode of action of a promising non-antibiotic citrus fruit extract against several pathogens. Front Microbiol 2019;10:884.
[71] Zhang L, Liu C, Li D, Zhao Y, Zhang X, Zeng X, et al. Antioxidant activity of an exopolysaccharide isolated from *Lactobacillus plantarum* C88. Int J Biol Macromol 2013;54:270–5.
[72] Adebayo-Tayo B, Fashogbon R. In vitro antioxidant, antibacterial, in vivo immunomodulatory, antitumor and hematological potential of exopolysaccharide produced by wild type and mutant *Lactobacillus delbureckii* subsp. bulgaricus. Heliyon 2020;6(2):e03268.
[73] Mandade R, Sreenivas S, Choudhury A. Radical scavenging and antioxidant activity of Carthamus tinctorius extracts. Free Radic Antioxid 2011;1 (3):87–93.
[74] de Torre MP, Cavero RY, Calvo MI, Vizmanos JL. A simple and a reliable method to quantify antioxidant activity in vivo. Antioxidants 2019;8(5):142.
[75] Samadian H, Zamiri S, Ehterami A, Farzamfar S, Vaez A, Khastar H, et al. Electrospun cellulose acetate/gelatin nanofibrous wound dressing containing berberine for diabetic foot ulcer healing: in vitro and in vivo studies. Sci Rep 2020;10(1):1–12.
[76] Ai A, Behforouz A, Ehterami A, Sadeghvaziri N, Jalali S, Farzamfar S, et al. Sciatic nerve regeneration with collagen type I hydrogel containing chitosan nanoparticle loaded by insulin. Int J Polym Mater Polym Bio 2019;68 (18):1133–41.
[77] Alimov I, Menon S, Cochran N, Maher R, Wang Q, Alford J, et al. Bile acid analogues are activators of pyrin inflammasome. J Biol Chem 2019;294 (10):3359–66.
[78] Ghalayani Esfahani A, Altomare L, Bonetti L, Nejaddehbashi F, Boccafoschi F, Chiesa R, et al. Micro-Structured Patches for Dermal Regeneration Obtained via Electrophoretic Replica Deposition. Appl Sci 2020;10(14):5010.
[79] Liu X-Z, Wang Q-M, Theelen B, Groenewald M, Bai F-Y, Boekhout T. Phylogeny of tremellomycetous yeasts and related dimorphic and filamentous basidiomycetes reconstructed from multiple gene sequence analyses. Stud Mycol 2015;81(1):1–26.
[80] Delattre C, Pierre G, Laroche C, Michaud P. Production, extraction and characterization of microalgal and cyanobacterial exopolysaccharides. Biotechnol Adv 2016;34(7):1159–79.
[81] Li H, Li J, Dou W, Shi J, Xu Z. Enhancing the production of a novel exopolysaccharide by *Bacillus mucilaginosus* CGMCC5766 Using Statistical experiment design. Trop J Pharm Res 2013;12(5):711–8.
[82] Oleksy M, Klewicka E. Exopolysaccharides produced by *Lactobacillus* sp.: Biosynthesis and applications. Crit Rev Food Sci Nutr 2018;58(3):450–62.
[83] Okoro OV, Gholipour AR, Sedighi F, Shavandi A, Hamidi M. Optimization of Exopolysaccharide (EPS) Production by *Rhodotorula mucilaginosa* sp. GUMS16. ChemEngineering 2021;5(3):39.
[84] Petersen G, Schubert W, Richards G, Nelson G. Yeasts producing exopolysaccharides with drag-reducing activity. Enzyme Microb Technol 1990;12(4):255–9.
[85] Ramirez M, Ramirez LV. Application of plackettburman screening design to enhance exopolysaccharide production from Rhodotorula yeast strains. J Soc Technol 2015;5(1):16–23.
[86] Lin E-S, Sung S-C. Cultivating conditions influence exopolysaccharide production by the edible *Basidiomycete Antrodia* cinnamomea in submerged culture. Int J Food Microbiol 2006;108(2):182–7.
[87] Guo MQ, Hu X, Wang C, Ai L. Polysaccharides: structure and solubility. Solubility of polysaccharides 2017;2:8–21.
[88] Freitas F, Alves VD, Pais J, Costa N, Oliveira C, Mafra L, et al. Characterization of an extracellular polysaccharide produced by a *Pseudomonas* strain grown on glycerol. Bioresour Technol 2009;100(2):859–65.

[89] Arvidson SA, Rinehart BT, Gadala-Maria F. Concentration regimes of solutions of levan polysaccharide from *Bacillus* sp. Carbohydr Polym 2006;65(2):144–9.
[90] Ramirez M. Characterization and safety evaluation of exopolysaccharide produced by *Rhodotorula minuta* BIOTECH 2178. Int J Food Eng 2016;2 (1):31–5.
[91] Bramhachari P, Kishor PK, Ramadevi R, Rao BR, Dubey SK. Isolation and characterization of mucous exopolysaccharide (EPS) produced by *Vibrio furnissii* strain VB0S3. J Microbiol Biotechnol 2007;17:44–51.
[92] Wilson R, Goodfellow B, Belton P. Fourier transform infrared spectroscopy for the study of food biopolymers. Food Hydrocolloids 1988;2(2):169–78.
[93] Okoro OV, Sun Z. The characterisation of biochar and biocrude products of the hydrothermal liquefaction of raw digestate biomass. Biomass Convers Biorefin 2021;11(6):2947–61.
[94] Kanamarlapudi SLRK, Muddada S. Characterization of Exopolysaccharide Produced by *Streptococcus thermophilus* CC30. Biomed Res Int 2017;2017:4201809.
[95] Castellane TCL, Campanharo JC, Colnago LA, Coutinho ID, Lopes ÉM, Lemos MVF, et al. Characterization of new exopolysaccharide production by *Rhizobium tropici* during growth on hydrocarbon substrate. Int J Biol Macromol 2017;96:361–9.
[96] Vasanthakumari DS, Harikumar S, Beena DJ, Pandey A, Nampoothiri KM. Physicochemical Characterization of an Exopolysaccharide Produced by a Newly Isolated *Weissella cibaria*. Appl Biochem Biotechnol 2015;176 (2):440–53.
[97] Shuhong Y, Meiping Z, Hong Y, Han W, Shan X, Yan L, et al. Biosorption of Cu^{2+}, Pb^{2+} and Cr^{6+} by a novel exopolysaccharide from *Arthrobacter* ps-5. Carbohydr Polym 2014;101:50–6.
[98] Wang Y, Ahmed Z, Feng W, Li C, Song S. Physicochemical properties of exopolysaccharide produced by *Lactobacillus kefiranofaciens* ZW3 isolated from Tibet kefir. Int J Biol Macromol 2008;43(3):283–8.
[99] Lakra AK, Domdi L, Tilwani YM, Arul V. Physicochemical and functional characterization of mannan exopolysaccharide from *Weissella confusa* MD1 with bioactivities. Int J Biol Macromol 2020;143:797–805.
[100] Pavlova K, Panchev I, Hristozova T. Physico-chemical characterization of exomannan from *Rhodotorula acheniorum* MC. World J Microbiol Biotechnol 2005;21(3):279–83.
[101] Vazquez-Rodriguez A, Vasto-Anzaldo XG, Barboza Perez D, Vázquez-Garza E, Chapoy-Villanueva H, García-Rivas G, et al. Microbial Competition of *Rhodotorula mucilaginosa* UANL-001L and E. coli increase biosynthesis of Non-Toxic Exopolysaccharide with Applications as a Wide-Spectrum Antimicrobial. Sci Rep 2018;8(1):798..
[102] Ayyash M, Abu-Jdayil B, Itsaranuwat P, Galiwango E, Tamiello-Rosa C, Abdullah H, et al. Characterization, bioactivities, and rheological properties of exopolysaccharide produced by novel probiotic *Lactobacillus plantarum* C70 isolated from camel milk. Int J Biol Macromol 2020;144:938–46.
[103] Chen H, Wang Z, Qu Z, Fu L, Dong P, Zhang X. Physicochemical characterization and antioxidant activity of a polysaccharide isolated from oolong tea. Eur Food Res Technol 2009;229(4):629–35.
[104] Tsiapali E, Whaley S, Kalbfleisch J, Ensley HE, Browder IW, Williams DL. Glucans exhibit weak antioxidant activity, but stimulate macrophage free radical activity. Free Radic Biol Med 2001;30(4):393–402.
[105] Zhu Y, Wang C, Jia S, Wang B, Zhou K, Chen S, et al. Purification, characterization and antioxidant activity of the exopolysaccharide from *Weissella cibaria* SJ14 isolated from Sichuan paocai. Int J Biol Macromol 2018;115:820–8.
[106] Ma W, Chen X, Wang B, Lou W, Chen X, Hua J, et al. Characterization, antioxidativity, and anti-carcinoma activity of exopolysaccharide extract from *Rhodotorula mucilaginosa* CICC 33013. Carbohydr Polym 2018;181:768–77.
[107] Xu R, Shen Q, Ding X, Gao W, Li P. Chemical characterization and antioxidant activity of an exopolysaccharide fraction isolated from *Bifidobacterium animalis* RH. Eur Food Res Technol 2011;232(2):231–40.
[108] Wang Z, Zhao Y, Jiang Y, Prebiotic CuW. Antioxidant, and Immunomodulatory Properties of Acidic Exopolysaccharide From Marine *Rhodotorula* RY1801. Front Nutr 2021;8(549).
[109] Mirzaei Seveiri R, Hamidi M, Delattre C, Rahmani B, Darzi S, Pierre G, et al. Characterization of the exopolysaccharides from *Rhodotorula minuta* IBRC-M 30135 and evaluation of their emulsifying, antioxidant and antiproliferative activities. Med Sci 2019;23(97):381–9.
[110] Raveendran S, Palaninathan V, Chauhan N, Sakamoto Y, Yoshida Y, Maekawa T, et al. In vitro evaluation of antioxidant defense mechanism and hemocompatibility of mauran. Carbohydr Polym 2013;98(1):108–15.
[111] Zhong C, Cao G, Rong K, Xia Z, Peng T, Chen H, et al. Characterization of a microbial polysaccharide-based bioflocculant and its anti-inflammatory and pro-coagulant activity. Colloids Surf B Biointerfaces 2018;161:636–44.
[112] Adan A, Kiraz Y, Baran Y. Cell Proliferation and Cytotoxicity Assays. Curr Pharm Biotechnol 2016;17(14):1213–21.
[113] Kibar H, Arslan YE, Ceylan A, Karaca B, Haliscelik O, Kiran F. *Weissella cibaria* EIR/P2-derived exopolysaccharide: A novel alternative to conventional biomaterials targeting periodontal regeneration. Int J Biol Macromol 2020;165:2900–8.
[114] Liu J-S, Zeng Y-X, Bi S-Y, Zhou J-W, Cheng R, Li J, et al. Characterization and chemical modification of PLN-1, an exopolysaccharide from *Phomopsis liquidambari* NJUSTb1. Carbohydr Polym 2021;253:117197.
[115] Wang J, Wu T, Fang X, Min W, Yang Z. Characterization and immunomodulatory activity of an exopolysaccharide produced by *Lactobacillus plantarum* JLK0142 isolated from fermented dairy tofu. Int J Biol Macromol 2018;115:985–93.
[116] Uhliariková I, Šutovská M, Barboríková J, Molitorisová M, Kim HJ, Park YI, et al. Structural characteristics and biological effects of exopolysaccharide produced by cyanobacterium *Nostoc* sp. Int J Biol Macromol 2020;160:364–71.
[117] Jiang P, Yuan L, Huang G, Wang X, Li X, Jiao L, et al. Structural properities and immunoenhancement of an exopolysaccharide produced by *Phellinus pini*. Int J Biol Macromol 2016;93:566–71.
[118] Trabelsi I, Ktari N, Slima SB, Triki M, Bardaa S, Mnif H, et al. Evaluation of dermal wound healing activity and in vitro antibacterial and antioxidant activities of a new exopolysaccharide produced by *Lactobacillus* sp. Ca_6. Int J Biol Macromol 2017;103:194–201.
[119] Ben Ayed H, Bardaa S, Moalla D, Jridi M, Maalej H, Sahnoun Z, et al. Wound healing and in vitro antioxidant activities of lipopeptides mixture produced by *Bacillus mojavensis* A21. Process Biochem 2015;50(6):1023–30.
[120] Lawrence WT. Physiology of the Acute Wound. Clin Plast Surg 1998;25 (3):321–40.
[121] Li R, Liu K, Huang X, Li D, Ding J, Liu B, et al. Bioactive Materials Promote Wound Healing through Modulation of Cell Behaviors. Adv Sci 2022;9 (10):2105152.
[122] Krzyszczyk P, Schloss R, Palmer A, Berthiaume F. The role of macrophages in acute and chronic wound healing and interventions to promote pro-wound healing phenotypes. Front Physiol 2018;9:419.
[123] Mapoung S, Umsumarng S, Semmarath W, Arjsri P, Thippraphan P, Yodkeeree S, et al. Skin wound-healing potential of polysaccharides from medicinal mushroom *Auricularia auricula*-judae (Bull.). J Fungi 2021;7(4):247..
[124] Jiang F, Ding Y, Tian Y, Yang R, Quan M, Tong Z, et al. Hydrolyzed low-molecular-weight polysaccharide from *Enteromorpha prolifera* exhibits high anti-inflammatory activity and promotes wound healing. Mater Sci Eng C 2021:112637.
[125] Koh TJ, DiPietro LA. Inflammation and wound healing: the role of the macrophage. Expert Rev Mol Med 2011;13:e23.
[126] Dipietro LA, Reintjes MG, Low QEH, Levi B, Gamelli RL. Modulation of macrophage recruitment into wounds by monocyte chemoattractant protein-1. Wound Repair Regen 2001;9(1):28–33.
[127] Xin Y, Ji H, Cho E, Roh K-B, You J, Park D, et al. Immune-enhancing effect of water-soluble beta-glucan derived from enzymatic hydrolysis of yeast glucan. Biochem Biophys Rep 2022;30:101256.
[128] Li Z, Bratlie KM. The Influence of Polysaccharides-Based Material on Macrophage Phenotypes. Macromol Biosci 2021;21(8):2100031.
[129] Mugade M, Patole M, Pokharkar V. Bioengineered mannan sulphate capped silver nanoparticles for accelerated and targeted wound healing: Physicochemical and biological investigations. Biomed Pharmacother 2017;91:95–110.
[130] Kikuchi S, Griffin CT, Wang S-S, Bissell DM. Role of CD44 in epithelial wound repair: migration of rat hepatic stellate cells utilizes hyaluronic acid and CD44v6. J Biol Chem 2005;280(15):15398–404.
[131] Wei Z, Huang L, Cui L, Zhu X. Mannose: Good player and assister in pharmacotherapy. Biomed Pharmacother 2020;129:110420.
[132] Gan J, Dou Y, Li Y, Wang Z, Wang L, Liu S, et al. Producing anti-inflammatory macrophages by nanoparticle-triggered clustering of mannose receptors. Biomaterials 2018;178:95–108.
[133] Hameedaldeen A, Liu J, Batres A, Graves GS, Graves DT. FOXO1, TGF-β regulation and wound healing. Int J Mol Sci 2014;15(9):16257–69.